Genome sequencing and CAZymes repertoire analysis of *Diaporthe eres* P3-1W causing 'Hongyang' postharvest rot in China (#97008)

First submission

Guidance from your Editor

Please submit by **5 Apr 2024** for the benefit of the authors (and your token reward) .

Structure and Criteria
Please read the 'Structure and Criteria' page for general guidance.

Custom checks
Make sure you include the custom checks shown below, in your review.

Author notes
Have you read the author notes on the guidance page?

Raw data check
Review the raw data.

Image check
Check that figures and images have not been inappropriately manipulated.

If this article is published your review will be made public. You can choose whether to sign your review. If uploading a PDF please remove any identifiable information (if you want to remain anonymous).

Files

Download and review all files from the materials page.

5 Figure file(s)
3 Table file(s)
1 Raw data file(s)
5 Other file(s)

Custom checks

DNA data checks

- Have you checked the authors data deposition statement?
- Can you access the deposited data?
- Has the data been deposited correctly?
- Is the deposition information noted in the manuscript?

Structure and Criteria

Structure your review

The review form is divided into 5 sections. Please consider these when composing your review:

1. **BASIC REPORTING**
2. **EXPERIMENTAL DESIGN**
3. **VALIDITY OF THE FINDINGS**
4. General comments
5. Confidential notes to the editor

You can also annotate this PDF and upload it as part of your review

When ready submit online.

Editorial Criteria

Use these criteria points to structure your review. The full detailed editorial criteria is on your guidance page.

BASIC REPORTING

- Clear, unambiguous, professional English language used throughout.
- Intro & background to show context. Literature well referenced & relevant.
- Structure conforms to PeerJ standards, discipline norm, or improved for clarity.
- Figures are relevant, high quality, well labelled & described.
- Raw data supplied (see PeerJ policy).

EXPERIMENTAL DESIGN

- Original primary research within Scope of the journal.
- Research question well defined, relevant & meaningful. It is stated how the research fills an identified knowledge gap.
- Rigorous investigation performed to a high technical & ethical standard.
- Methods described with sufficient detail & information to replicate.

VALIDITY OF THE FINDINGS

- Impact and novelty not assessed. *Meaningful* replication encouraged where rationale & benefit to literature is clearly stated.
- All underlying data have been provided; they are robust, statistically sound, & controlled.
- Conclusions are well stated, linked to original research question & limited to supporting results.

Standout reviewing tips

The best reviewers use these techniques

Tip	*Example*
Support criticisms with evidence from the text or from other sources	*Smith et al (J of Methodology, 2005, V3, pp 123) have shown that the analysis you use in Lines 241-250 is not the most appropriate for this situation. Please explain why you used this method.*
Give specific suggestions on how to improve the manuscript	*Your introduction needs more detail. I suggest that you improve the description at lines 57- 86 to provide more justification for your study (specifically, you should expand upon the knowledge gap being filled).*
Comment on language and grammar issues	*The English language should be improved to ensure that an international audience can clearly understand your text. Some examples where the language could be improved include lines 23, 77, 121, 128 – the current phrasing makes comprehension difficult. I suggest you have a colleague who is proficient in English and familiar with the subject matter review your manuscript, or contact a professional editing service.*
Organize by importance of the issues, and number your points	*1. Your most important issue* *2. The next most important item* *3. …* *4. The least important points*
Please provide constructive criticism, and avoid personal opinions	*I thank you for providing the raw data, however your supplemental files need more descriptive metadata identifiers to be useful to future readers. Although your results are compelling, the data analysis should be improved in the following ways: AA, BB, CC*
Comment on strengths (as well as weaknesses) of the manuscript	*I commend the authors for their extensive data set, compiled over many years of detailed fieldwork. In addition, the manuscript is clearly written in professional, unambiguous language. If there is a weakness, it is in the statistical analysis (as I have noted above) which should be improved upon before Acceptance.*

Genome sequencing and CAZymes repertoire analysis of *Diaporthe eres* P3-1W causing ‘Hongyang’ postharvest rot in China

Li-Zhen Ling [1], **Ling-Ling Chen** [1, 2], **Zhen-Zhen Liu** [1], **Lan-Ying Luo** [1], **Si-Han Tai** [1], **Shu-Dong Zhang** [Corresp. 1]

[1] School of Biological Sciences and Technology, Liupanshui Normal University, Liupanshui, Guizhou, China

[2] College of Life and Health, Dalian University, Dalian, Liaoning, China

Corresponding Author: Shu-Dong Zhang
Email address: sdchang@foxmail.com

Kiwifruit postharvest rot caused by several fungal pathogens, is one of the most destructive diseases that leads to the tremendous economic loss in kiwifruit industry worldwide. In this study, we first isolated the strain P3-1W as a causal agent of ‘Hongyang’ postharvest rot disease in China and identified as *Diaporthe eres* based on the morphological and molecular data. To further understand pathogenic mechanism, we sequenced the genome of this strain using PacBio and Illumina sequencing technologies. The resultant assembly revealed the genome of *D. eres* P3-1W had a total length of 58,489,835 bp, with N50 of 5,939,879 bp and 50.7% GC content. 15,407 total protein-coding genes (PCGs) were predicted and functionally annotated using the different public databases. The genome analysis of *D. eres* P3-1W showed a total of 857 carbohydrate-active enzymes (CAZymes), one of the virulence factors were identified and shared the general characteristics with seven other *Diaporthe* species albeit of the different numbers. The CAZymes repertoires of these *Diaporthe* genomes all were divided into six classes: glycoside hydrolases (GHs), carbohydrate esterases (CEs), polysaccharide lyases (PLs), glycosyltransferases (GTs), and auxiliary activities (AA) and carbohydrate binding modules (CBMs). And the CAZymes included 12 AAs, 68 GHs, 30 GTs, 7 PLs, 10 CEs, and 24 CBMs in *D. eres* P3-1W genome. In addition, four cell wall polysaccharide-disassembling enzymes, including cellulase, β-galactosidase, polygalacturonase and pectin methylesterases showed a significant peak of enzymic activities at the second day after *D. eres* P3-1W infection. The results of this study provide useful resources for further exploration of the complicated pathogenic mechanisms in *D. eres* P3-1W.

Genome sequencing and CAZymes repertoire analysis of *Diaporthe eres* P3-1W causing 'Hongyang' postharvest rot in China

Li-Zhen Ling [1], Ling-Ling Chen [1,2], Zhen-Zhen Liu, Lan-Ying Luo[1], Si-Han Tai[1] and Shu-Dong Zhang [1,*]

[1] School of Biological Sciences and Technology, Liupanshui Normal University, Liupanshui, Guizhou, 553004

[2] College of Life and Health, Dalian University, Dalian, 116622

Corresponding Author:

Shu-Dong Zhang

Minghu Road, Liupanshui, Guizhou, 553004, China

Email address: sdchang@foxmail.com

Abstract

Kiwifruit postharvest rot caused by several fungal pathogens, is one of the most destructive diseases that leads to the tremendous economic loss in kiwifruit industry worldwide. In this study, we first isolated the strain P3-1W as a causal agent of 'Hongyang' postharvest rot disease in China and identified as *Diaporthe eres* based on ~~the~~ morphological and molecular data. To further understand pathogenic mechanism, we sequenced the genome of this strain using PacBio and Illumina sequencing technologies. The resultant assembly revealed the genome of *D. eres* P3-1W had a total length of 58,489,835 bp, with N50 of 5,939,879 bp and 50.7% GC content. 15,407 total protein-coding genes (PCGs) were predicted and functionally annotated ~~using the different public databases~~. The genome analysis of *D. eres* P3-1W showed a total of 857 carbohydrate-active enzymes (CAZymes), one of the virulence factors were identified and shared the general characteristics with seven other *Diaporthe* species albeit of the different numbers. The CAZymes repertoires of these *Diaporthe* genomes all were divided into six classes:

glycoside hydrolases (GHs), carbohydrate esterases (CEs), polysaccharide lyases (PLs), glycosyltransferases (GTs), and auxiliary activities (AA) and carbohydrate binding modules (CBMs). And the CAZymes included 12 AAs, 68 GHs, 30 GTs, 7 PLs, 10 CEs, and 24 CBMs in *D. eres* P3-1W genome. In addition, four cell wall polysaccharide-disassembling enzymes, including cellulase, β-galactosidase, polygalacturonase and pectin methylesterases showed a significant peak of enzymic activities at the second day after *D. eres* P3-1W infection. The results of this study provide useful resources for further exploration of the complicated pathogenic mechanisms in *D. eres* P3-1W.

Introduction

Kiwifruit is an economically important fruit crop in the genus *Actinidia* of Actinidiaceae family. China ~~has become~~ the center of the diversity of kiwifruit~~. For example~~, approximately 52 *Actinidia* species ~~have been identified in China~~ (Huang 2016). Kiwifruit began the demonstration history in the early 20th century when the wild seeds from China were transferred into New Zealand (Ferguson 1984). To date, numerous cultivation varieties have been developed, in which *A. chinensis* and *A. chinensis* var. *deliciosa* are two most commercial kiwifruit varieties (Waswa et al. 2024). 'Hongyang' (*A. chinensis*) is the first cultivar with a red-flesh inner pericarp, which derived from clonally selected wild germplasm in central China (Zhen et al. 2004). 'Hongyang' has received considerable attention over the last forty years and is widely grown in China because of delicious taste and high nutritional components (vitamin C, minerals, carotenoids and anthocyanins) (Wang et al. 2021a).

~~However,~~ 'Hongyang' is highly susceptible to soft rot disease during cultivation and postharvest storage, which results in the significant economic loss each year and has become a serious problem to threaten its industry (Jiqing et al. 2019; Ling et al. 2023b). It has documented that several fungal pathogens from the genera *Botrytis*, *Diaporthe* and *Alternaria* can cause fruit rot during storage (Li et al. 2017a; Ling et al. 2023b). Among these pathogens, *Botrytis* sp. and *Diaporthe* sp. have always been considered the most important pathogens for stored kiwifruit. At present, the major strategy to control these pathogens is dependent on the environmentally harmful fungicides, which can lead to persistent residues of fungicides in the fruit and the increasing risk of antifungal resistance development (Bardas et al. 2010). Alternative method is the application of biocontrol agents (i.e. yeast) against several postharvest pathogens (Francesco

et al. 2016). The efficacy of these controlling pathogen strategies is mainly attributed to different action mechanisms, such as the production of antifungal compounds and cell wall degrading enzymes (CWDEs) ~~and so on~~. In order to reduce the impact of this destructive disease, an increased understanding of the pathogenicity mechanisms of the responsible species is of vital importance.

The complete genome sequences of the causal agents provide the basic information to explore their pathogenicity. ~~At present, a wide variety of different next generation sequencing (NGS) technologies are now available (Di Bella et al. 2013). For example, Illumina's HiSeq can produce a number of short reads with a high sequencing depth at comparatively low costs, which exhibits mean error rates < 1% (Laehnemann et al. 2016). However, the assembly problem needs to be overcome because the short reads often have shown the complex repeats.~~ Alternatively, the third-generation sequencing platform Pacific Bioscience (PacBio) using single-molecule real-time (SMRT) sequencing technology can provide the longer reads over 20 kb to overcome the assembly problems associated with short reads. However, lower sequencing depth and higher error rates have reported in this platform (Laehnemann et al. 2016). Therefore, combination of PacBio and HiSeq reads provides the improvements in assembly contiguity and per-base accuracy (Laehnemann et al. 2016). ~~Our recent study has shown that the complete genome of *Alternaria tenuissima* P1-2W, a new causal agent of 'Hongyang' soft rot disease has achieved the high quality of assembly at the chromosome level (Ling et al. 2023a).~~

Plant cell wall is the first barrier against pathogen attack and is largely comprised of polysaccharides (i.e. hemicellulose, cellulose and pectin) (Chen et al. 2018). Carbohydrate Active Enzymes (CAZymes) secreted by ~~the~~ pathogens ~~always~~ perform the breakdown of ~~the~~ cell wall polysaccharides and often regarded as one of pathogenic factors (Castillo et al. 2017). These enzymes have been classified into six categories by carbohydrate-active enzyme (CAZy) database: auxiliary activity (AA), carbohydrate esterase (CE), and carbohydrate-binding modules (CBMs), glycoside hydrolase (GH), glycosyl transferase (GT), polysaccharide lyases (PL) (Drula et al. 2022). In recent years, genome sequencing has revealed a large number of candidates for CAZymes have been extensively described for many pathogenic species (Castillo et al. 2017). The pathogenicity of these fungus has reported to be associated with cell wall degrading enzymes (CWDEs) during infection. An array of CWDEs, such as cellulase (Cx), β-galactosidase (β-Gal), polygalacturonase (PG) and pectin methylesterases (PME), can induce the

disassembly of cell wall polysaccharides, which is beneficial to pathogen infection (Ramos et al. 2016). Changes in these CWDE activities were associated with the disease development in some plants, such as Longyan (Chen et al. 2018), apples (Miedes & Lorences 2006), grapefruits (Shi et al. 2019), pumpkin (Li et al. 2023).

In this study, a pathogenic strain P3-1W was isolated from the diseased 'Hongyang' fruit with a typical rot symptom. ~~And~~ the genome of P3-1W was then sequenced and assembled by a combination of Illumina NovaSeq and PacBio SMRT sequencing technologies. Finally, genome-wide identification of CAZymes-encoding genes were performed, and the activities of several CAZymes genes such as Cx, β-Gal, PG and PME were investigated during the different P3-1W infecting stages. Therefore, description of genome coupled with the enzyme assay results will contribute to the understanding of the underlying mechanisms of pathogenicity of the strain P3-1W.

Materials & Methods

Pathogen isolation and pathogenicity test

'Hongyang' fruits with typical symptoms of rot were collected from a cold storage in Liupanshui City of Guizhou Province. The pathogen was obtained and purified from the diseased fruit by a routine tissue isolation method as previously described (Ling et al. 2023b). To evaluate the potential as pathogens of 'Hongyang' soft rot disease, mycelial plugs (5 mm in diameter) of the pathogen obtained from potato dextrose agar (PDA) media were placed on the surface of fresh healthy kiwifruits, which were incubated at 25 °C in the dark until the rot symptomatic tissues were observed. The pathogen was re-isolated from the diseased tissues. Sterile PDA plugs with the same size was used as control. Three trials were conducted, and each time included 5 fruits.

Pathogen identification

The pathogenic strain was identified with both morphological and molecular methods. For morphological identification, the strain was cultured on PDA media at 25 °C for 3 days. For molecular identification, the DNA of the pathogen was extracted with the fungal DNA isolation kit (Sangon Biotech, Shanghai, China) according to the manufacture' protocol. Internal transcribed spacer (ITS) and translation elongation factor 1 (*TEF1*) gene segments were amplified, and the primers of each segment were described in Table S1. The polymerase chain reaction (PCR) system contained 12.5 μL 2 × Taq PCR mix, 0.4 μL each primer (10 μmol L^{-1}), 1

μL DNA template, and 8.2 μL double distilled water. PCR reaction was used the following programs: initial denaturation at 95 ℃ for 3 min, following by 35 cycles of denaturation at 95 ℃ for 20 s, annealing 58 ℃ for 30 s and extension at 72 ℃ for 1 min and a final extension at 72 ℃ for 5 min. The resultant PCR product was sequenced by Sangon Biotech.

ITS (PP256503) and *TEF1* segments (Table S2) were use for phylogenetic analysis [23]. The corresponding sequences from 86 *Diaporthe* species were downloaded from NCBI database (Table S3). Two loci sequences were concatenated to a single alignment dataset for phylogenetic inference using maximum likelihood analysis (ML). The phylogenetic tree was conducted using RAxML v7.2.6 (Stamatakis 2006) under GTRGAMMA model for 1000 bootstraps (Drummond et al. 2012).

Genomic DNA Extraction and Sequencing

~~The pathogenic strain P3-1W was cultured on PDA media at 25 °C in the dark for 4 days.~~ Up to 100 mg the mycelia of pathogen were collected from the Petri dishes and frozen with liquid nitrogen. The genomic DNA of the pathogen was extracted with DNeasy Plant Kit (Qiagen, Hilden, Germany) following the protocol provided by the manufacture. The quality of DNA was measured with Nanodrop 2000c (Thermo Scientific, Wilmington, USA).

For Illumina sequencing platform, the 350 bp paired-end library was constructed according to the manufacturer's introductions (Illumina) and sequenced on the Illumina Novaseq 6000 platform by Berry Genomics Company (http://www.berrygenomics.com/. Beijing, China). Basically, the libraries were prepared following these steps: DNA fragmentation by sonication, end-polishing of the DNA fragments, A-tailing and ligation with the full-length adapters for Illumina sequencing, PCR amplification, and purification of PCR products (AMPure XP bead system). The libraries were analyzed for size distribution using an Agilent 2100 Bioanalyzer.

PacBio SMRT bell library preparation was performed using the procedure as follows: (1) 7 μg high quality genomic DNA was evaluated using pulsed-field electrophoresis, most of DNA fragments should be longer than 20 Kb. (2) DNA was sheared with mode size of 40 Kb or larger using g-TUBE (Covaris 520079). (3) AMPure® PB Beads was used to concentrate DNA (Pacific Biosciences 100-265-900). (4) SMRTbell library was prepared using the Kit 2.0. Single-Strand overhangs was removed, and then we performed DNA damage reparation, end-repair, A-tailing, adapter ligation and Enzymatic digestion. At last, Library size-selection was conducted by

SageELF (Sage Science ELF000). (5). After library size selection, the library was prepared for sequencing for 15/30 hours on the Sequel II/IIe system (Pacific Biosciences, CA, USA).

Genome assembly and annotation

Illumina sequencing reads were first used to ~~make a survey to~~ estimate genome size and heterozygosity with Jellyfish (Hesse 2023) and GenomeScope (Ranallo-Benavidez et al. 2020). After filtering the low-quality reads, the clean reads were used to *de novo* assemble into contigs and scaffolds with SOAPdenovo software (Bankevich et al. 2012). The genome assemble quality was assessed by Benchmarking Universal Single-Copy Orthologues (BUSCO) (Simão et al. 2015). The assembled genome was scanned using RepeatMasker (Tarailo-Graovac & Chen 2009) to mask the repeat sequences and annotate TEs. The prediction of protein-coding genes (PCGs) was performed with Funannotate (https://github.com/nextgenusfs/funannotate). tRNA and rRNA genes were identified using tRNAscan-SE and BAsic Rapid Ribosomal RNA Predictor (barrnap), respectively. Rfam was used to annotate the snRNAs with the default parameters. The functional annotation of PCGs was performed by BLASTP against NR (https://blast.ncbi.nlm.nih.gov/Blast.cgi), COG (https://www.ncbi.nlm.nih.gov/COG/), GO (http://geneontology.org/) and KEGG (http://www.genome.jp/kegg/).

Identification of CAZymes genes and comparative analysis

Carbohydrate-active enzyme (CAZyme) searches against Pfam Hidden Markov Models (HMMs) were performed using HMMER 3.0 package (http://hmmer.org/) available from dbCAN database (Zheng et al. 2023). DIAMOND was used for fast blast hits in the CAZy database.

Eight additional fungal genomes were included for comparative analyses. *D. amygdali* CAA958, *D. eres* CBS 160.32, *D. capsici*, *D. citri* ZJUD2, *D. citriasiana* ZJUD30, *P. longicolla*, *D. batatatis*, and *D. phragmitis* NJD1. Of them, *D. phragmitis* NJD1 was one of causal agent of kiwifruit rot (Wang et al. 2021b) and used to perform a comparison of the characteristics of genome. Seven other genomes were used to compare the abundance of CAZymes and these species used in this study were mainly pathogens of soybean (Li et al. 2017b), citrus (Gai et al. 2021), grapevine (Morales-Cruz et al. 2015), blueberry (Hilário et al. 2022), sunflower (Baroncelli et al. 2016), walnut (Fang et al. 2020) and sweet potato (Yang et al. 2022).

Crude enzyme extraction and assay of enzyme activity

The strain P3-1W was cultured on PDA media for strain activation. Mycelial plugs (5 mm) were cut from the edge of a 3-day-old colony of the strain and transferred to the surface of 'Hongyang' fruit with 4 or 5 small wounds. ~~The~~ blank PDA plug with the same size was established as the negative control group. After inoculation, the fruits were sealed and incubated under the dark conditions and disease progression was monitored. Then, the lesion margins between infected and healthy fruit were collected each day after inoculation for examining enzyme activity.

Crude enzyme was extracted based on the ~~procedures described by~~ Chen' method (Chen et al. 2018) with some modifications. Briefly, three grams of fresh fruit tissue were homogenized with 12 mL of 2 M NaCl buffer solution (including 10 mmoL/L EDTA and 5 g/L PVP) adjusted to pH 7.4 using Tris-HCl, at 4 °C. Then homogenate was centrifuged at 15000 × g for 30 min at 4 °C. The supernatant was used as the crude enzymatic extract.

The enzyme activities of cellulase (Cx), PG and PME was determined with 3,5-dinitrosalicylic acid (DNS) colorimetric method. The reaction mixture contained 1.0 ml substrate solution and 1.0 ml of sodium acetate buffer (pH 4.4) and the reaction was initiated by adding 0.5 ml of crude enzyme, following by incubation at 37 °C for 30 min. A volume of 1.5 mL of DNS was then added to the reaction mixture after the reaction was terminated by boiling for 5 min and the OD values of reducing production were measured at 540 nm. The reaction mixture by adding boiled crude enzyme was used as the blank. The experiments were repeated at least three times. The substrates for Cx, PG, and PME were 1% (w/w) carboxymethyl cellulose, 1.0% (m/v) polygalacturonic acid and 1.0% (m/v) pectin, respectively. The PG and PME activities were expressed as reducing units (RU). One RU was defined as the amount of enzyme required to release reducing groups at 1 μmol/min using D-galacturonic acid as standard. By contrast, one unit (U) of cellulase activity was defined as the micromoles of glucose released per minute of reaction using glucose as standard.

β-galactosidase (β-Gal) activity was determined in a reaction mixture including 5.0 mL of 20 mmol sodium acetate (pH 4.7), 2ml of 3 mmol/L p-nitrophenyl-β--D-galactopyranoside, and 1.0 mL of crude enzyme. The reaction was incubated at 37 °C for 30 min. A volume of 2 mL of 0.2 mmol/L Na_2CO_3 was then added to the mixture to stop the reaction. The concentration of the reducing product was determined at 420 nm with p-nitrophenol (PNP) as a standard. One unit of β-Gal activity referred to the amount of enzyme that produced 1 mmol PNP per hour.

Results

Isolation and identification of pathogen

The fungal isolate P3-1W was obtained from the diseased fruit of 'Hongyang' using the tissue isolation method. After incubation, the colony of this strain was round and cream-like on PDA media, with a white surface, while the back turned brown (Figure 1A and B). To confirm the pathogenicity of this strain, the healthy 'Hongyang' fruits with 4 to 5 pinholes were inoculated by mycelial plugs (5 mm in diameter) of the strain P3-1W from PDA media and the sterile PDA plug was applied as the negative control treatment. At the fifth day of inoculation, the fruits inoculated with mycelial plugs of P3-1W showed the obvious symptom of soft rot, whereas the control remained asymptomatic (Figure 1C and D). Moreover, the strain was successful reisolated from the diseased fruits of 'Hongyang', which the morphological characters was consistent with that of the strain P3-1W. Therefore, the strain P3-1W was confirmed as the causal agent responsible for 'Hongyang' soft rot disease in this study. The sequences of internal transcribed spacer (ITS) and translation elongation factor 1 (*TEF1*) of this strain were amplified to construct the phylogenetic tree. Phylogenetic analysis revealed that the strain of P3-1W was clustered into one clade with *D. eres* (Figure S1). Therefore, the strain P3-1W was identified as *D. eres*.

The genome characteristics of *D. eres* P3-1W

In this study, the genome sequence of *D. eres* P3-1W was obtained using a combination of two sequencing platforms. Illumina platform first generated 242.15 × and 97,013,864 paired-end short reads (Table 1). These short reads were processed for quality control and adapter trimming, and the resultant clean reads were used to reveal the overall genome characteristics of *D. eres* P3-1W. Based on Kmer analysis, the genome size was estimated at 58.9 Mb, with a heterozygosity ratio of 17.5%. In addition, we performed the sequencing of PacBio long reads (~20 kb). Approximately 613,696 subreads (about 12 Gb, ~208 ×) were generated and the lengths of mean and N50 subreads were 19,950 bp and 22,159 bp, respectively (Table 1). *De novo* assembly of *D. eres* P3-1W genome was achieved using SOAPdenovo software and a total of 14 scaffolds were obtained. The assembled genome of *D. eres* P3-1W was 58,489,835 bp in size, with N50 of 5,939,879 bp and 50.7% GC content (Table 2). In addition, we estimated the completeness of genome assembly using BUSCO, and found that this genome included 97.6% of the conserved core genes sets (Table 2). By contrast, *D. phragmitis* NJD1 was found to cause the

kiwifruit soft rot and its genome sequenced by Illumina and PacBio has been released (Wang et al. 2021b). Its genome has contained 28 contigs with a contig N50 of 3,550,333 bp (Table 2). Apparently, the genome assembly of *D. eres* P3-1W in this study had a higher quality than that of *D. phragmitis* NJD1.

A total of 1,473,598 bp of the repetitive sequences were identified with RepeatMasker (Tarailo-Graovac & Chen 2009), accounting for 2.52% of *D. eres* P3-1W genome (Table 2). The masked genome sequence was used for the *ab initio* gene prediction. A total of 15,407 protein-coding genes (PCGs) with the mean length of 1,584 bp were predicted in *D. eres* P3-1W genome (Table 2). And the number of tRNA and rRNA genes was 143 and 45, respectively (Table 2). In addition, 23 non-coding RNA genes were identified in the genome of *D. eres* P3-1W (Table 2). To further determine the functions of these PCGs, 97.28% out of 15,407 PCGs were functionally annotated in the different databases as listed in Table 2. Our results revealed that 14,988 genes had significant sequence similarity with orthologous proteins in NCBI-NR database. In addition, 6,003 PCGs were assigned to COG categories (Figure 2), in which the most abundant category was “Carbohydrate metabolism and transport”, followed by “Secondary Structure”. Among three GO classifications, the commonest molecular functions of PCGs were “binding” and “catalytic activity”; in terms of biological process, the majority were associated with “cellular processes” and “metabolic processes”; three most abundant cellular components were “cell”, “organelle” and “membranes” (Figure S2). To further identify the biological pathways of these PCGs, we performed KEGG pathway analysis. In total, 2,979 genes were annotated in the KEGG database (Table 2), in which “global view and maps” was the most enriched term, followed by “amino acid metabolism” and “Carbohydrate metabolism” (Figure S3). This annotated functions of PCGs in *D. eres* P3-1W were similar to those in *D. phragmitis* NJD1 had the similar annotation except for COG and KEGG pathway in the big difference in gene number (Table 2).

The identification of CAZyme genes in *D. eres* P3-1W genome

In the present study, annotation of *D. eres* P3-1W genome using the dbCAN database revealed a total of 857 genes were identified to encode for putative CAZymes, accounting for 5.49% of the predicted genes (Table 2 and Figure 3). The distribution of CAZymes in *D. eres* P3-1W and seven other fungi species was showed in Figure 3. The results demonstrated that the total number of CAZymes ranged from 857 in *D. eres* P3-1W and *D. amygdali* up to 1,580 in *D. citri* ZJUD2 (Figure 3). All six classes of CAZymes were detected in these species’ genomes and

glycoside hydrolases (GHs) and auxiliary activities (AAs) were the two groups with the most abundant predicted proteins (Figure 3). ~~Four other CAZymes showed the different distribution in all analyzed species.~~ For example, 142 CBMs were identified in *D. capsici*, but only 20 ones in *D. amygdali*. Relatively speaking, the number of PLs showed the smallest change in six classes of CAZymes (Figure 3). Among these species, the member number of each CAZyme family in *D. eres* P3-1W was the most similar to that of in *D. eres* CBS 160.32.

In *D. eres* P3-1W genome, GHs was the largest CAZymes family and 374 genes belonging to 68 different subfamilies were made up 43.64% of CAZymes repertoire (Figure 3 and 4). The main subfamilies were GH43 (34), GH5 (26), GH3 (23), GH18 (17), GH28 (16), GH16 (16) and GH13 (15) (Figure 4A). In addition, a vast array of genes was associated with cellulase (GH3, -5, -6, -7, -12, and -45), pectinase (GH28), hemicellulose (GH11 and GH43), xylanase (GH10, -11, and -30) and chitinase (GH18) in the genome of *D. eres* P3-1W. In the present study, CAZyme annotation revealed that *D. eres* P3-1W contained a total of 11 AA families with 221 AAs in its genome sequence (Figure 4B). Cellobiose dehydrogenases (AA3) subfamily was prominent, with 74 members, and xylo- and cello-oligosaccharide oxidases (AA7) subfamily was the second largest subfamily with 57 AAs in *D. eres* P3-1W genome (Figure 4B). Carbohydrate esterase (CE) family classification also revealed that the majority of CEs were CE10 subfamily members (50), followed by CE5 members (18) (Figure 4C). In addition, 30 genes predicted to encode PLs were identified and belonged to 7 subfamilies (Figure 4D). Of them, pectase lyases PL1 was the most prominent subfamily, 3 subfamilies (PL11, -26, -27) with only one gene were identified in the genome of P3-1W (Figure 4D). Among GT family, GT32 and GT71 subfamilies were the most abundant (Figure 4E). However, CBMs were the smallest family of CAZymes and only 24 members were found in the genome, in which CBM50 was the most abundant subfamily (Figure 4F).

The activity of four enzymes during inoculation of *D. eres* P3-1W

In this study, the activities of β-galactosidase (β-Gal), cellulase (Cx), polygalacturonase (PG) and pectin methylesterase (PME) were detected during the different stages of *D. eres* P3-1W inoculation and the raw data were shown in Table S4. As can be seen in Figure 5, four enzymes except β-Gal showed the similar trends during *D. eres* P3-1W infection. The activities of these three enzymes began to increase after inoculation and reached their maximum activities at the second day after inoculation (dpi), and declined from 3 dpi, and then increased at 5 dpi (Figure

5A, B and C). The activities of these enzymes during *D. eres* P3-1W inoculation were significantly higher than the control at the same infection time. By contrast, the activity of β-Gal showed ~~the little~~ difference from those of three above enzymes. ~~Similarly~~, its activities significantly increased in the first two days after P3-1W inoculation, then sharply declined from 3 dpi. ~~Especially~~, the activity of β-Gal was decreased to the level of control at the fifth dpi (Figure 5D).

Discussion

In this study, we isolated *Diaporthe* strain P3-1W as the causal agent of "Hongyang" postharvest rot disease. Previous studies have documented that many *Diaporthe* species have been ~~frequently~~ reported as plant pathogenic fungi and are responsible for diseases of economically important plants (Santos et al. 2017). It is evident that many fungi in the genus *Diaporthe* can cause plant ulcers, leaf blight, cankers, branch blight, leaf spot, shoot dieback, fruit rot, root rot, and bark necrosis (Chaisiri et al. 2021; Fang et al. 2020; Simão et al. 2015). Currently, the taxonomy of *Diaporthe* primarily based on molecular data combined with morphological characterization and host associations (Abramczyk et al. 2023; Santos et al. 2017). In the early years, one ITS segment as the official fungal barcode (Mathew et al. 2015; Ménard et al. 2014) can identify the *Diaporthe* species but now at least two loci segments (i.e. ITS and *TEF1*) are used to identify this genus species due to the actively changing taxonomy of *Diaporthe* (Santos et al. 2017). In this study, our results indicated that the strain P3-1W was identified as *D. eres* based on ITS and *TEF1* segments. Previous studies have shown that *Diaporthe* species, including *D. phragmitis* (Wang et al. 2021b), *Phomopsis longicolla* (Liu et al. 2020), *D. perniciosa*, *D. actinidiae* (Lee 2001), *D. ambigua* (Auger et al. 2013), *D. novem* (Díaz et al. 2014), *D. australafricana*, *D. rudis* (Díaz et al. 2017), *D. lithocarpus* (Li et al. 2016) and *D. viticola* (Luongo 2011) have caused the kiwifruit soft rot or fruit decays. In recent years, *D. eres* has been reported in association with fruit rot in hardy kiwifruit in China (Liu et al. 2021a) and *A. deliciosa* kiwifruit in South Korea (Park et al. 2023). Therefore, *D. eres* as a causal agent was first reported in the 'Hongyang' kiwifruit in China.

In past decades, the studies on *Diaporthe* mostly focused on the identification of plant pathogens, endophytic fungi, and their metabolites (Strobel et al. 2011; Tanney et al. 2016). In recent years, numerous next-generation sequencing (NGS) technologies are now available, providing cheaper, faster, and higher-throughput sequencing. The third-generation sequencing

platform PacBio RS II has been successfully applied in the genome sequencing of many pathogenic *Diaporthe* species, such as *D. citri* (Liu et al. 2021b), *D.* phragmitis (Wang et al. 2021b), *P. longicolla* (Zhao et al. 2021), *D. ilicicola* (Emanuel et al. 2022). In addition, high confidence reads from Illumina can be used to correct the errors inherent in PacBio sequences. Therefore, hybrid assemblies use the combined approaches of PacBio and Illumina sequencing technologies to yield improvements in assembly contiguity and per-base accuracy (Laehnemann et al. 2016). To date, the genome-sequencing studies have been performed to reveal the pathogenicity-related genes (candidate effectors, cellular transporters, biosynthetic metabolite gene clusters (BGCs), and CAZymes) in the pathogenic strains (Hilário et al. 2022; Li et al. 2017b; Park et al. 2018). In the present study, we obtained a high-quality genome sequence of *D. eres* P3-1W. Functional annotation of this genome revealed that the genes involved in "Carbohydrate metabolism and transport" were the most abundant. And then, we focused on the analysis of CAZymes that are often involved in pathogenicity and have received attention because of their colonization of plant host by degrading plant cell wall.

For the pathogenic fungi, the successful infection means can break the barriers of plant cell wall by degenerating polysaccharides, such as cellulose, beta-glucans, hemicellulose, and pectin. A variety of CAZymes are involved in the degeneration of these abovementioned polysaccharides components and widely found in plant pathogenic fungi (Castillo et al. 2017). In this study, the high-quality genome sequence of *D. eres* P3-1W had 857 CAZymes, which were classified into 68 subfamilies of GHs, 30 subfamilies of GTs, 10 subfamilies of CEs, 12 subfamilies of AAs, and 7 subfamilies of PLs genes. Meanwhile, our results indicated that six CAZymes families were identified in other *Diaporthe* species, indicating the presence of all CAZymes families might become the general features of this genus species. Previous study has revealed that the genes encoding pectinase (GH28), cellulase (GH3 and GH12) and hemicellulose (GH11 and GH43) in GHs family are related to *Valsa Mali* infecting apple (Silva et al. 2020). In this study, a vast array of genes associated with cellulase (GH3, -5, -6, -7, -12, and -45), pectinase (GH28), hemicellulose (GH11 and GH43), xylanase (GH10, -11, and -30) and chitinase (GH18) were found in the genome sequence of *D. eres* P3-1W. Based on the results, we speculate that *D. eres* P3-1W might possess the potential to degrade these substrates as a major source of carbon in nature. Meanwhile, these results indicated that these genes might play an important role in *D. eres* P3-1W pathogenicity.

To further validate our hypotheses, we examined the activities of four enzymes (PG, PME, β-Gal and Cx) in this study. PG and PME are two major enzymes to digest pectin that is a complex polysaccharide present in the middle lamella of plant cell walls (Patidar et al. 2018). Moreover, previous studies have shown that ~~only~~ PG enzymes do not sufficiently degrade pectin and the synergistic action PG and PME enzymes can accelerate the depolymerization of pectin (Li et al. 2019). Our results indicated that the activities of PG and PME were significantly enhanced by *D. eres* P3-1W treatment, suggesting that *D. eres* P3-1W infection promoted the depolymerization and dissolution of pectin. Meanwhile, the activities of Cx, an enzyme of degrading cellulose as well as β-Gal were prompted by P3-1W. Therefore, these results suggested that *D. eres* P3-1W infection can cause a significant increase in the activities of CWDEs. In this study, CWDEs is a big family, and an array of candidate genes were identified. However, which member was associated with the pathogenicity of *D. eres* P3-1W? Which member plays the major role in the pathogenicity of *D. eres* P3-1W? These questions need to be studied in the future.

Conclusions

In this study, *D. eres* P3-1W was first reported as a causal agent of 'Hongyang' kiwifruit postharvest rot disease. The genome of *D. eres* P3-1W was sequenced by combination of Illumina and PacBio sequencing technology. The size of the genome was 58,489,835 bp, with N50 of 5,939,879 bp and 50.7% GC content. Among predicted 15,407 PCGs, a total of 857 CAZymes were identified and included 12 AAs, 68 GHs, 30 GTs, 7 PLs, 10 CEs, and 24 CBMs in *D. eres* P3-1W genome. Moreover, the activities of Cx, β-Gal, PG and PME were apparently promoted by *D. eres* P3-1W infection. Therefore, description of genome coupled with the enzyme assay results will contribute to the understanding of the underlying mechanisms of pathogenicity of *D. eres* P3-1W.

Supplementary Materials: Figure S1: The ML phylogenetic tree of P3-1W and 86 other *Diaporthe* species based on ITS and TEF1; Figure S2: GO categories assigned to PCGs of P3-1W genome; Figure S3: KEGG pathway annotation of PCGs of P3-1W. Table S1: Primer sets and corresponding amplification targets; Table S2: TEF1 sequences of *D. eres* P3-1W; Table S3: The *Diaporthe* species used in the construction of phylogenetic tree; Table S4: The raw data of the activity of four enzymes (Cx, β-Gal, PG and PME).

Author Contributions: Conceptualization, S-D.Z. and L-Z.L.; methodology, L-L.C., Z-Z.L., L-Y.L., S-H.T.; formal analysis, L-Z.L. and S-D.Z.; data curation, L-Z.L. and S-D.Z.; writing—original draft preparation, L-Z.L.; writing—review and editing, S-D.Z.; funding acquisition, L-Z.L. All authors have read and agreed to the published version of the manuscript.

Funding: This work was supported by Guizhou Science and Technology Department, grant number QianKeHeJiChu-ZK[2022]530 and the Scientific Research (Cultivation) Project of Liupanshui Normal University, grant number LPSSY2023KJZDPY06.

Data Availability Statement: The genome raw data was deposited in the NCBI database with BioProject accession number PRJNA1073476, BioSample accession number SAMN3983127 and SRA accession number SRR27880200 (for illumina data) and SRR28059423 (for PacBio data).

Conflicts of Interest: The authors declare no conflict of interest.

References

Abramczyk B, Pecio Ł, Kozachok S, Kowalczyk M, Marzec-Grządziel A, Król E, Gałązka A, and Oleszek W. 2023. Pioneering metabolomic studies on *Diaporthe eres* species complex from fruit trees in the south-eastern Poland. *Molecules* 28. 10.3390/molecules28031175

Auger J, Pérez I, and Esterio M. 2013. *Diaporthe ambigua* associated with post-harvest fruit rot of kiwifruit in Chile. *Plant Dis* 97:843-843. 10.1094/PDIS-10-12-0990-PDN

Bankevich A, Nurk S, Antipov D, Gurevich AA, Dvorkin M, Kulikov AS, Lesin VM, Nikolenko SI, Pham S, Prjibelski AD, Pyshkin AV, Sirotkin AV, Vyahhi N, Tesler G, Alekseyev MA, and Pevzner PA. 2012. SPAdes: a new genome assembly algorithm and its applications to single-cell sequencing. *J Comput Biol* 19:455-477. 10.1089/cmb.2012.0021

Bardas GA, Veloukas T, Koutita O, and Karaoglanidis GS. 2010. Multiple resistance of *Botrytis cinerea* from kiwifruit to SDHIs, QoIs and fungicides of other chemical groups. *Pest Manag Sci* 66:967-973. 10.1002/ps.1968

Baroncelli R, Scala F, Vergara M, Thon MR, and Ruocco M. 2016. Draft whole-genome sequence of the *Diaporthe helianthi* 7/96 strain, causal agent of sunflower stem canker. *Genom Data* 10:151-152. 10.1016/j.gdata.2016.11.005

Castillo L, Plaza V, Larrondo LF, and Canessa P. 2017. Recent advances in the study of the plant pathogenic fungus *Botrytis cinerea* and its interaction with the environment. *Curr Protein Pept Sci* 18:976-989. 10.2174/1389203717666160809160915

Chaisiri C, Liu XY, Yin WX, Luo CX, and Lin Y. 2021. Morphology characterization, molecular phylogeny, and pathogenicity of *Diaporthe passifloricola* on *Citrus reticulata* cv. *Nanfengmiju* in Jiangxi province, China. *Plants (Basel)* 10. 10.3390/plants10020218

Chen Y, Zhang S, Lin H, Sun J, Lin Y, Wang H, Lin M, and Shi J. 2018. *Phomopsis longanae Chi*-induced changes in activities of cell wall-degrading enzymes and contents of cell wall components in pericarp of harvested longan fruit and its relation to disease development. *Front Microbiol* 9:1051. 10.3389/fmicb.2018.01051

Di Bella JM, Bao Y, Gloor GB, Burton JP, and Reid G. 2013. High throughput sequencing methods and analysis for microbiome research. *J Microbiol Methods* 95:401-414. 10.1016/j.mimet.2013.08.011

Díaz GA, Latorre BA, Jara S, Ferrada E, Naranjo P, Rodríguez J, and Zoffoli JP. 2014. First report of *Diaporthe novem* causing postharvest rot of kiwifruit during controlled atmosphere storage in Chile. *Plant Dis* 98:1274-1274. 10.1094/PDIS-02-14-0183-PDN

Díaz GA, Latorre BA, Lolas M, Ferrada E, Naranjo P, and Zoffoli JP. 2017. Identification and characterization of *Diaporthe ambigua*, *D. australafricana*, *D. novem*, and *D. rudis* causing a postharvest fruit rot in kiwifruit. *Plant Dis* 101:1402-1410. 10.1094/PDIS-10-16-1535-RE

Drula E, Garron ML, Dogan S, Lombard V, Henrissat B, and Terrapon N. 2022. The carbohydrate-active enzyme database: functions and literature. *Nucleic Acids Res* 50:D571-d577. 10.1093/nar/gkab1045

Drummond AJ, Suchard MA, Xie D, and Rambaut A. 2012. Bayesian phylogenetics with BEAUti and the BEAST 1.7. *Mol Biol Evol* 29:1969-1973. 10.1093/molbev/mss075

Emanuel IB, Konkel ZM, Scott KL, Valero David GE, Slot JC, and Peduto Hand F. 2022. Whole-genome sequence data for the holotype strain of *Diaporthe ilicicola*, a fungus associated with latent fruit rot in deciduous holly. *Microbiol Resour Announc* 11:e0063122. 10.1128/mra.00631-22

Fang X, Qin K, Li S, Han S, Zhu T, Fang X, and Qin K. 2020. Whole genome sequence of *Diaporthe capsici*, a new pathogen of walnut blight. *Genomics* 112:3751-3761. 10.1016/j.ygeno.2020.04.018

Ferguson AR. 1984. Kiwifruit: a botanical review. *John Wiley & Sons, Inc*.

Francesco AD, Martini C, and Mari M. 2016. Biological control of postharvest diseases by microbial antagonists: how many mechanisms of action? *European Journal of Plant Pathology* 145:711-717.

Gai Y, Xiong T, Xiao X, Li P, Zeng Y, Li L, Riely BK, and Li H. 2021. The genome sequence of the *Citrus* melanose pathogen *Diaporthe citri* and two *Citrus*-related *Diaporthe* species. *Phytopathology* 111:779-783. 10.1094/phyto-08-20-0376-sc

Hesse U. 2023. K-Mer-based genome size estimation in theory and practice. *Methods Mol Biol* 2672:79-113. 10.1007/978-1-0716-3226-0_4

Hilário S, Gonçalves MFM, Fidalgo C, Tacão M, and Alves A. 2022. Genome analyses of two blueberry pathogens: *Diaporthe amygdali* CAA958 and *Diaporthe eres* CBS 160.32. *J Fungi (Basel)* 8:804. 10.3390/jof8080804

Huang H. 2016. Chapter 3 - Natural distribution of genus *Actinidia*. In: Huang H, ed. *Kiwifruit*. San Diego: Academic Press, 169-190.

Jiqing L, Wenneng W, Ying L, Xiuqin L, Weijie L, and Rui W. 2019. Identification of pathogen isolation and pathogenicity difference of 'HongYang' kiwifruit ripe rot in Liupanshui city,Guizhou province. *Northern Horticulture* 4:31-38.

Laehnemann D, Borkhardt A, and McHardy AC. 2016. Denoising DNA deep sequencing data-high-throughput sequencing errors and their correction. *Brief Bioinform* 17:154-179. 10.1093/bib/bbv029

Lee JG, Lee, D.-H., Park, S.-Y., Hur, J.-S., and Koh, Y.-J. 2001. First report of *Diaporthe actinidiae*, the causal organism of stem-end rot of kiwifruit in Korea. *Plant Pathol J*:110-113.

Li L, Pan H, Chen M, Zhang S, and Zhong C. 2017a. Isolation and identification of pathogenic fungi causing postharvest fruit rot of kiwifruit (*Actinidia chinensis*) in China. *Journal of Phytopathology* 165:782–790.

Li L, Pan H, Chen MY, and Zhong CH. 2016. First report of *Diaporthe lithocarpus* causing postharvest rot of kiwifruit in Sichuan province, China. *Plant Dis* 100:2327-2327. 10.1094/PDIS-04-16-0488-PDN

Li S, Darwish O, Alkharouf NW, Musungu B, and Matthews BF. 2017b. Analysis of the genome sequence of *Phomopsis longicolla*: a fungal pathogen causing *Phomopsis* seed decay in soybean. *BMC Genomics* 18:688. 10.1186/s12864-017-4075-x

Li T, Shi D, Wu Q, Yin C, Li F, Shan Y, Duan X, and Jiang Y. 2019. Mechanism of cell wall polysaccharides modification in harvested 'Shatangju' mandarin (*Citrus reticulate Blanco*) fruit caused by *Penicillium italicum*. *Biomolecules* 9. 10.3390/biom9040160

Li W, Jiang Y, Hu C, Liu G, Li Y, and Wang S. 2023. Identification, pathogenic mechanism and control of *Rhizopus oryzae* causing postharvest fruit rot in pumpkin. *Postharvest Biology and Technology* 204:112460. https://doi.org/10.1016/j.postharvbio.2023.112460

Ling L-Z, Liu Z-Z, and Zhang S-D. 2023a. Genome sequence of *Alternaria tenuissima* P1-2W infecting postharvest kiwifruit. *PhytoFrontiers™* 3:902-905. 10.1094/PHYTOFR-07-23-0085-A

Ling L, Chen L, Tu D, and Zhang S. 2023b. Isolation and identification of pathogenic fungi causing fruit rot of hongyang kiwifruit during cold storage. *Anhui Agricultural Science Bulletin* 29:114-118.

Liu H, Pang L, Lu X, Wang R, and Zhou Q. 2020. First report of phomopsis longicolla associated with postharvest fruit rot of kiwifruit in China. *Plant Dis* 104:579.

505 Liu J, Guo X, Zhang H, Cao Y, and Sun Q. 2021a. First report of postharvest fruit rot disease of
506 hardy kiwifruit caused by *Diaporthe eres* in China. *Plant Dis* 105:3745. 10.1094/pdis-08-
507 20-1705-pdn
508 Liu XY, Chaisiri C, Lin Y, Yin WX, and Luo CX. 2021b. Whole-genome sequence of *Diaporthe*
509 *citri* isolate NFHF-8-4, the causal agent of *Citrus* melanose. *Mol Plant Microbe Interact*
510 34:845-847. 10.1094/mpmi-01-21-0004-a
511 Luongo L, Santori, A., Riccioni, L., and Belisario, A. 2011. *Phomopsis* sp. associated with post-
512 harvest fruit rot of kiwifruit in Italy. *J Plant Pathol*:205-209.
513 Mathew FM, Rashid KY, Gulya TJ, and Markell SG. 2015. First report of phomopsis stem
514 canker of sunflower (*Helianthus annuus*) caused by *Diaporthe gulyae* in Canada. *Plant*
515 *Dis* 99:160. 10.1094/pdis-08-14-0858-pdn
516 Ménard L, Brandeis PE, Simoneau P, Poupard P, Sérandat I, Detoc J, Robbes L, Bastide F,
517 Laurent E, Gombert J, and Morel E. 2014. First report of umbel browning and stem
518 necrosis caused by *Diaporthe angelicae* on carrot in France. *Plant Dis* 98:421.
519 10.1094/pdis-06-13-0673-pdn
520 Miedes E, and Lorences EP. 2006. Changes in cell wall pectin and pectinase activity in apple and
521 tomato fruits during *Penicillium* expansum infection. *J Sci Food Agric* 86:1359-1364.
522 https://doi.org/10.1002/jsfa.2522
523 Morales-Cruz A, Amrine KC, Blanco-Ulate B, Lawrence DP, Travadon R, Rolshausen PE,
524 Baumgartner K, and Cantu D. 2015. Distinctive expansion of gene families associated
525 with plant cell wall degradation, secondary metabolism, and nutrient uptake in the
526 genomes of grapevine trunk pathogens. *BMC Genomics* 16:469. 10.1186/s12864-015-
527 1624-z
528 Park GG, Kim W, and Yang KY. 2023. Rapid and sensitive detection of the causal agents of
529 postharvest kiwifruit rot, *Botryosphaeria dothidea* and *Diaporthe eres*, using a
530 recombinase polymerase amplification assay. *Plant Pathol J* 39:522-527.
531 10.5423/ppj.nt.07.2023.0094
532 Park YJ, Jeong YU, and Kong WS. 2018. Genome sequencing and carbohydrate-active enzyme
533 (CAZyme) repertoire of the white rot fungus *Flammulina elastica*. *Int J Mol Sci* 19.
534 10.3390/ijms19082379
535 Patidar MK, Nighojkar S, Kumar A, and Nighojkar A. 2018. Pectinolytic enzymes-solid state
536 fermentation, assay methods and applications in fruit juice industries: a review. *3 Biotech*
537 8:199. 10.1007/s13205-018-1220-4
538 Ramos AM, Gally M, Szapiro G, Itzcovich T, Carabajal M, and Levin L. 2016. In vitro growth
539 and cell wall degrading enzyme production by *Argentinean* isolates of *Macrophomina*
540 *phaseolina*, the causative agent of charcoal rot in corn. *Rev Argent Microbiol* 48:267-273.
541 https://doi.org/10.1016/j.ram.2016.06.002

542 Ranallo-Benavidez TR, Jaron KS, and Schatz MC. 2020. GenomeScope 2.0 and Smudgeplot for
543 reference-free profiling of polyploid genomes. *Nat Commun* 11:1432. 10.1038/s41467-
544 020-14998-3
545 Santos L, Alves A, and Alves R. 2017. Evaluating multi-locus phylogenies for species
546 boundaries determination in the genus *Diaporthe*. *PeerJ* 5:e3120. 10.7717/peerj.3120
547 Shi Z, Yang H, Jiao J, Wang F, Lu Y, and Deng J. 2019. Effects of graft copolymer of chitosan
548 and salicylic acid on reducing rot of postharvest fruit and retarding cell wall degradation
549 in grapefruit during storage. *Food Chem* 283:92-100.
550 https://doi.org/10.1016/j.foodchem.2018.12.078
551 Silva MG, de Curcio JS, Silva-Bailão MG, Lima RM, Tomazett MV, de Souza AF, Cruz-Leite
552 VRM, Sbaraini N, Bailão AM, Rodrigues F, Pereira M, Gonçales RA, and de Almeida
553 Soares CM. 2020. Molecular characterization of siderophore biosynthesis in
554 *Paracoccidioides brasiliensis*. *IMA Fungus* 11:11. 10.1186/s43008-020-00035-x
555 Simão FA, Waterhouse RM, Ioannidis P, Kriventseva EV, and Zdobnov EM. 2015. BUSCO:
556 assessing genome assembly and annotation completeness with single-copy orthologs.
557 *Bioinformatics* 31:3210-3212. 10.1093/bioinformatics/btv351
558 Stamatakis A. 2006. RAxML-VI-HPC: maximum likelihood-based phylogenetic analyses with
559 thousands of taxa and mixed models. *Bioinformatics* 22:2688-2690.
560 10.1093/bioinformatics/btl446
561 Strobel G, Singh SK, Riyaz-Ul-Hassan S, Mitchell AM, Geary B, and Sears J. 2011. An
562 endophytic/pathogenic *Phoma* sp. from creosote bush producing biologically active
563 volatile compounds having fuel potential. *FEMS Microbiol Lett* 320:87-94.
564 10.1111/j.1574-6968.2011.02297.x
565 Tanney JB, Mcmullin DR, Green BD, Miller JD, and Seifert KA. 2016. Production of antifungal
566 and antiinsectan metabolites by the *Picea* endophyte *Diaporthe maritima* sp. *nov*. *Fungal*
567 *Biol* 120:1448-1457.
568 Tarailo-Graovac M, and Chen N. 2009. Using RepeatMasker to identify repetitive elements in
569 genomic sequences. *Curr Protoc Bioinformatics* Chapter 4:4.10.11-14.10.14.
570 10.1002/0471250953.bi0410s25
571 Wang S, Qiu Y, and Zhu F. 2021a. Kiwifruit (*Actinidia* spp.): A review of chemical diversity
572 and biological activities. *Food Chem* 350:128469. 10.1016/j.foodchem.2020.128469
573 Wang X, Dong H, Lan J, Liu Y, Liang K, Lu Q, Fang Z, and Liu P. 2021b. High-quality genome
574 resource of the pathogen of *Diaporthe* (*Phomopsis*) phragmitis causing kiwifruit soft rot.
575 *Mol Plant Microbe Interact* 34:218-221. 10.1094/mpmi-08-20-0236-a
576 Waswa EN, Ding S-X, Wambua FM, Mkala EM, Mutinda ES, Odago WO, Amenu SG, Muthui
577 SW, Linda EL, Katumo DM, Waema CM, Yang J-X, and Hu G-W. 2024. The genus
578 *Actinidia* Lindl. (Actinidiaceae): A comprehensive review on its ethnobotany,
579 phytochemistry, and pharmacological properties. *Journal of Ethnopharmacology*
580 319:117222. https://doi.org/10.1016/j.jep.2023.117222

581 Yang Y, Yao X, Xhang X, Zou H, Chen J, Fang B, and Huang L. 2022. Draft genome sequence
582 of *Diaporthe batatatis* causing dry rot disease in sweetpotato. *Plant Dis* 106:737-740.
583 10.1094/pdis-07-21-1530-a
584 Zhao X, Zhang Z, Zheng S, Ye W, Zheng X, and Wang Y. 2021. Genome sequence resource of
585 *Phomopsis longicolla* YC2-1, a fungal pathogen causing *Phomopsis* stem blight in
586 soybean. *Mol Plant Microbe Interact* 34:842-844. 10.1094/mpmi-12-20-0340-a
587 Zhen Y, Li Z, Huang H, and Wang Y. 2004. Molecular characterization of kiwifruit (*Actinidia*)
588 cultivars and selections using ssr markers. *Journal of the American Society for*
589 *Horticultural Science* 129:374-382.
590 Zheng J, Ge Q, Yan Y, Zhang X, Huang L, and Yin Y. 2023. dbCAN3: automated carbohydrate-
591 active enzyme and substrate annotation. *Nucleic Acids Res* 51:W115-w121.
592 10.1093/nar/gkad328
593

Figure 1

The colony morphology of strain P3-1W isolated from diseased ‘Hongyang’ fruits:

The colony morphology of strain P3-1W isolated from diseased ‘Hongyang’ fruits: (A) the front of colony and (B) the back of colony and symptoms of soft rot in ‘Hongyang’ fruit artificially inoculated mycelial plugs of P3-1W (C) and control (D) for 5 days after inoculation.

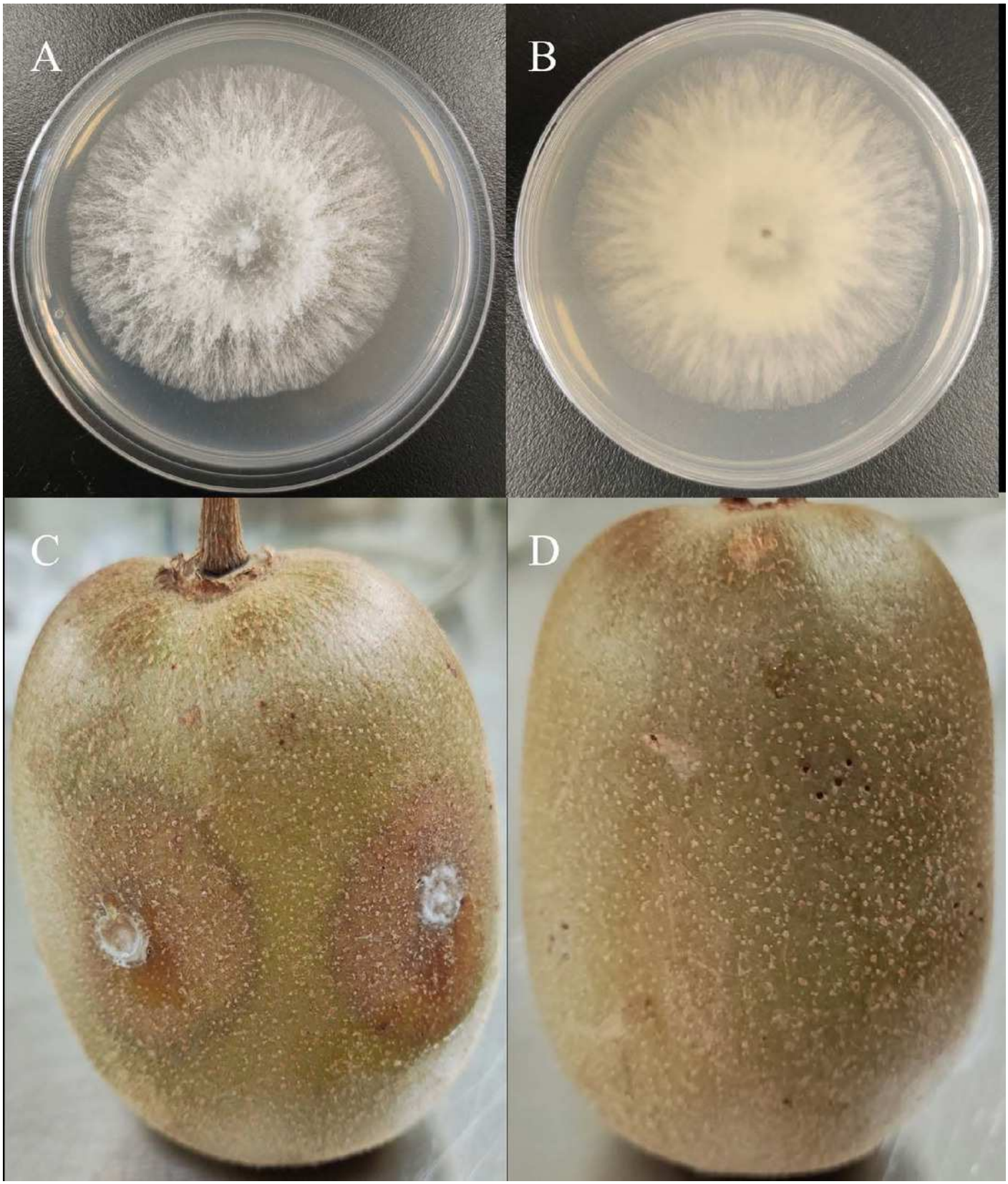
A
B
C
D

Figure 2

COG categories assigned to the PCGs of *D. eres* P3-1W genome

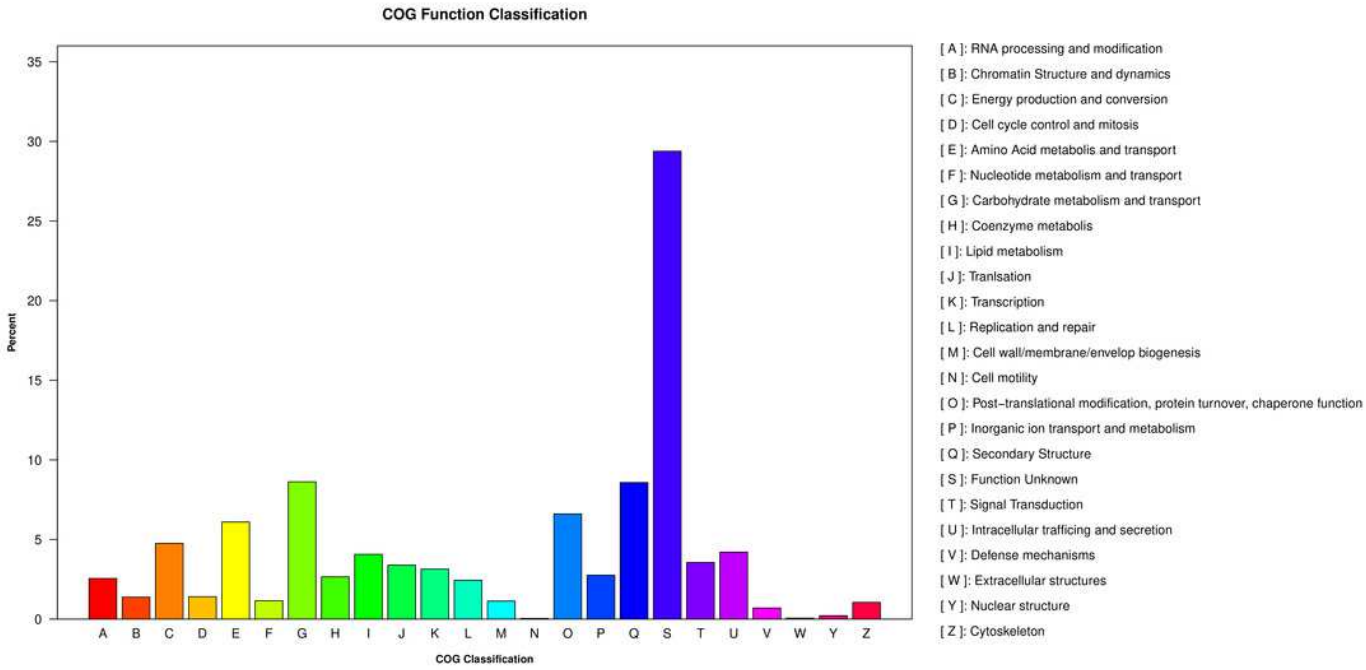

Figure 3

Comparative analysis of CAZymes in *D. eres* P3-1W and seven other *Diaporthe* species

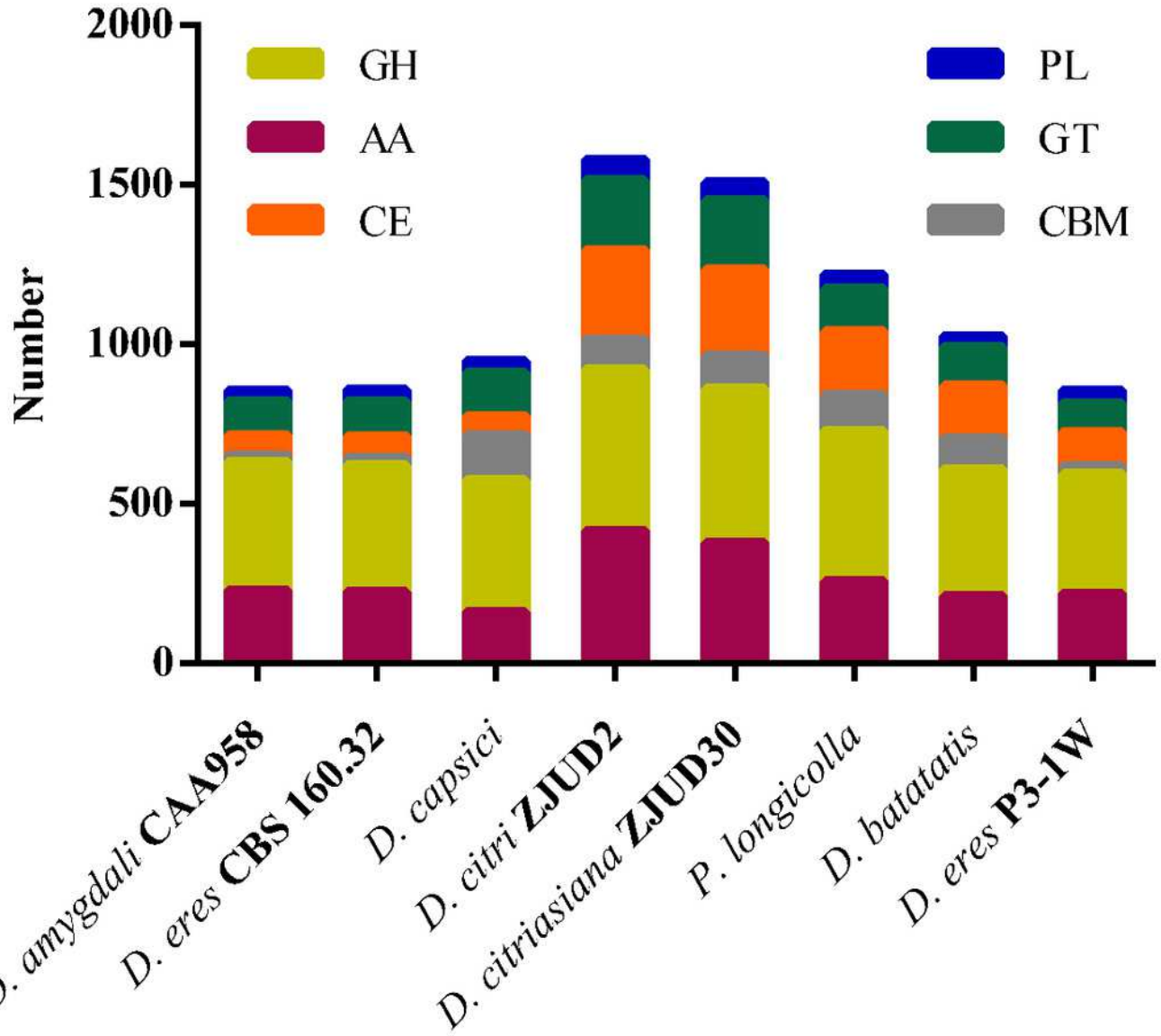

Figure 4

Number of CAZymes in *D. eres* P3-1W genome.

Number of CAZymes in *D. eres* P3-1W genome. Number of (A) GHs subfamilies; (B) AAs subfamilies; (C) CMBs subfamilies; (D) CEs subfamilies; (E) GTs subfamilies and (F) PLs subfamilies

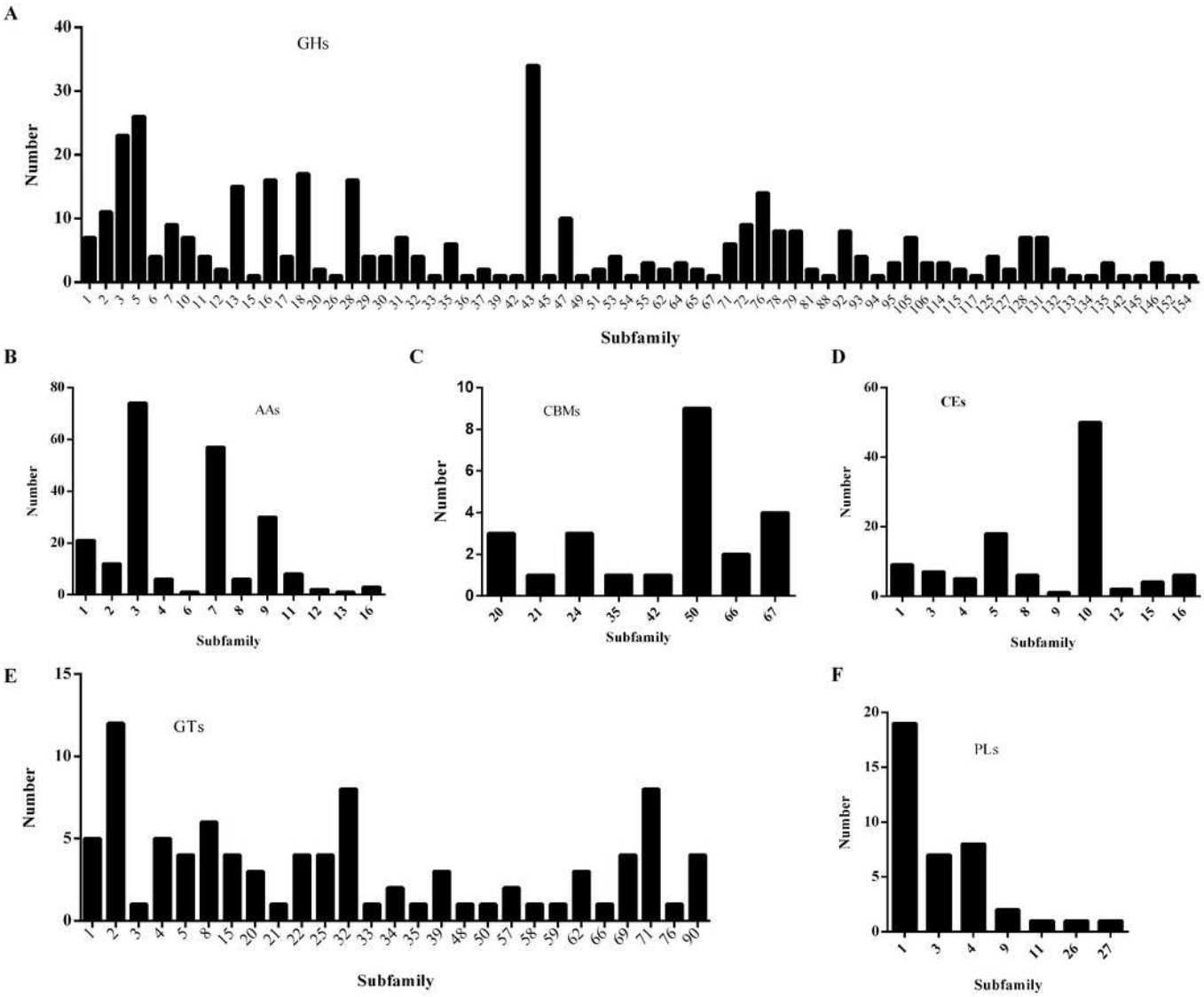

Figure 5

The activities of CWDEs during the different infection time of *D. eres* P3-1W.

The activities of CWDEs during the different infection time of *D. eres* P3-1W. Activity of (A) Cx; (B) PG; (C) PME and (D) β-Gal.

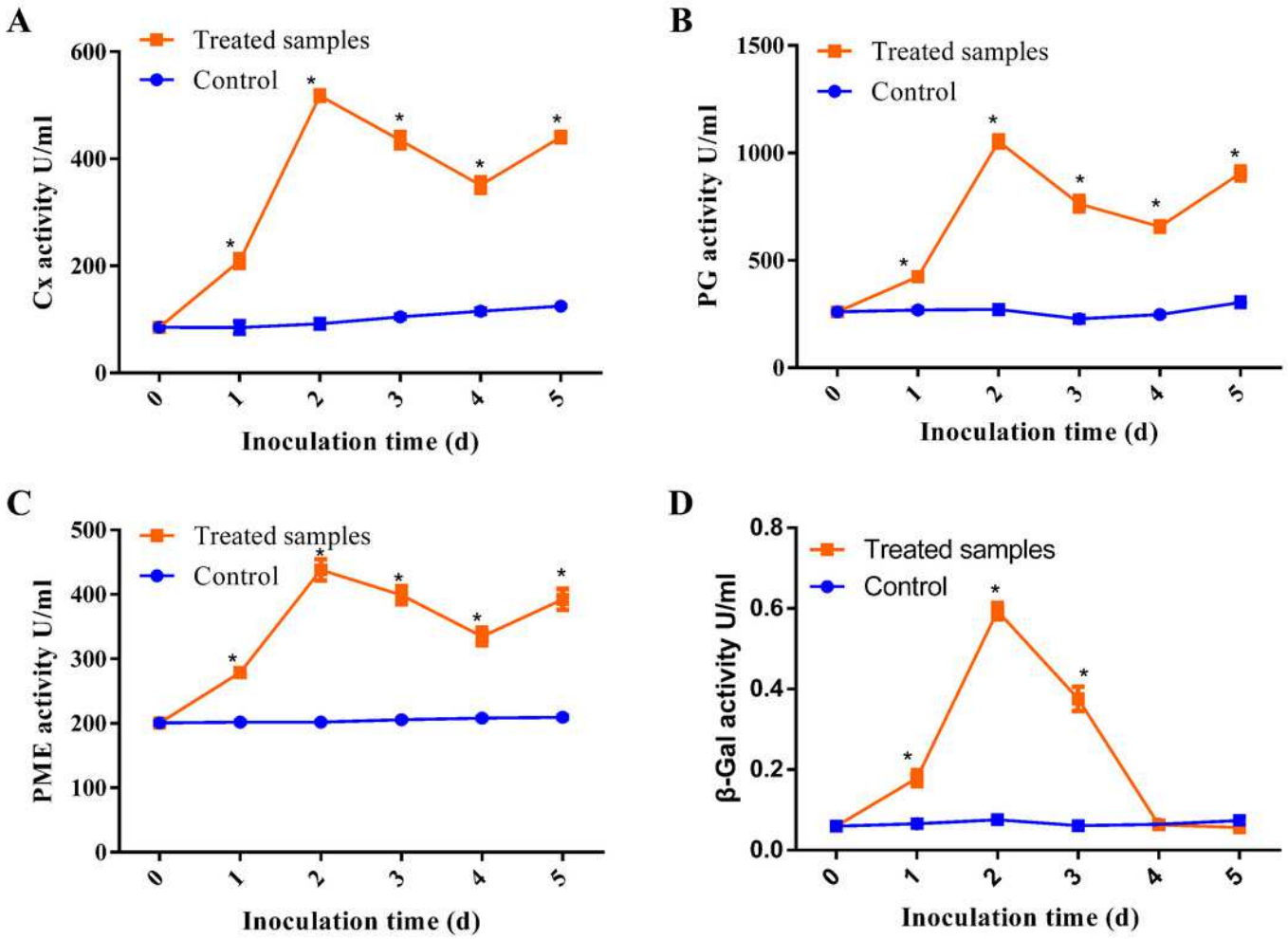

Table 1(on next page)

Table 1 Genome sequencing statistics of *D. eres* P3-1W

Table 1. Genome sequencing statistics of *D. eres* P3-1W

Illumina	Total reads	97,013,864
	Coverage	242.15 ×
	Raw data	14,552,079,600 bp
	Clean data	13,901,222,433 bp
	Estimated size	58.9 Mb
	Heterozygosity	17.5%
PacBio	Subreads bases	12,243,480,442 bp
	Coverage	208.78 ×
	Subreads reads	613,696
	Subreads Mean Length	19,950 bp
	Subreads N50	22,159 bp

Table 2(on next page)

Table 2 The genome features of *D. eres* P3-1W compared with *D. phragmitis* NJD1

Table 2. The genome features of *D. eres* P3-1W compared with *D. phragmitis* NJD1

	D. eres P3-1W	*D. phragmitis* NJD1
Genome size (bp)	58,489,835	58,328,132
GC%	50.7	50.82
N50 (bp)	5,939,879	3,550,333
Number of scaffolds/contigs	14	28
Repeat sequence (bp)	1,473,598	/
Total genes	15,618	12,393
PCGs	15,407	12393
ncRNAs	23	16
rRNAs	45	37
tRNAs	143	174
CAZymes	857	806
Genome BUSCO%	97.64	97.90
NR annotation	14,988	11,624
COG annotation	6,003	2,206
GO annotation	7,656	7,853
KEGG	2,979	10,207